Materials Research Bulletin 45 (2010) 1996–2000

Contents lists available at ScienceDirect

Materials Research Bulletin

journal homepage: www.elsevier.com/locate/matresbu

Reducing ultra-low thermal expansion of β-$Zr_2O(PO_4)_2$ by substitutions?

Céline Barreteau, Damien Bregiroux, Guillaume Laurent, Gilles Wallez *

UPMC Univ. Paris 06, CNRS-UMR 7574, ENSCP-ParisTech, Laboratoire de Chimie de la Matière Condensée de Paris, 11 rue Pierre et Marie Curie, 75231 Paris Cedex 05, France

ARTICLE INFO

Article history:
Received 21 July 2010
Accepted 16 August 2010
Available online 26 August 2010

Keywords:
A. Ceramics
A. Structural Materials
B. Sol–gel chemistry
C. X-ray diffraction
D. Thermal expansion

ABSTRACT

The ultra-low thermal expansion of β-$Zr_2O(PO_4)_2$ could still be reduced by chemical modifications, according to previous works on uranium and thorium IV homologues that evidenced a contracting effect of big cations. However, the present study shows that the only isovalent cations likely to substitute for Zr^{IV} or P^{V} are either harmful, or unstable, chemically or thermally. Furthermore, aliovalent modifications seem to be forbidden by the crystal structure of the material, leaving probably very few perspectives of improvement. Vanadium however improves significantly the crystallinity of the material and lowers the α–β transition temperature.

1. Introduction

Oxides with low or negative thermal expansion (L/NTE) make a small but remarkable class of materials. The formers, endowed with a high resistance to thermal shocks, have been used since the beginning of the XXth century for various high temperature applications, while the latters can be used to elaborate zero-expansion composites and constitute an original field of investigation for the academic. Research and design in this domain have long been ruled by empirical considerations and, as pointed by Roy et al. in 1989, progresses remained slow due to a limited understanding of the real causes of thermal contraction [1]. However, at the end of the following decade, thanks to the improvements of diffraction techniques, the pioneer works of Sleight led to a phenomenological classification in which the thermal evolutions of the polyhedra networks appeared as key parameters to understand the contraction mechanisms [2].

At this time, the anhydrous zirconium phosphates had been extensively studied by ceramists who evidenced remarkable LTE materials [3,4]. A high chemical and thermal stability, low toxicity, moderate cost and easiness of elaboration strongly contributed to the interest for these materials.

ZrP_2O_7 (cubic) (Fig. 1a) shows a 3 × 3 × 3-fold superstructure that collapses at high temperature. Above the transition point, this diphosphate [5] and its divanadate counterpart [6] show respectively LTE and NTE that result from the thermal rocking of the corner-connected ZrO_6 and P/VO_4 polyhedra.

The NZP family (from rhombohedral archetype $NaZr_2(PO_4)_3$) (Fig. 1b) gathers countless formulations through substitution of any size-compatible mono- or multivalent cation for Na^+ in the so-called *M*1 sixfold coordinated site. Iso- and aliovalent substitutions for Zr^{4+} in octahedral site and P^{5+} in tetrahedral site are also possible. The *M*2 sites, vacant in the archetype at room temperature, can be occupied by supplementary low-valence cations like Na^+, thus still extending the spectrum of chemical compositions. Driven by inter-cations Coulombic repulsions, the strong thermal expansion along the *c*-axis is balanced through a ring-like deformation mode by a contraction along the perpendicular axes [7,8].

The structure and low expansion mechanism of α-$Zr_2O(PO_4)_2$ (Fig. 1c) have been characterized only recently [9,10], but this metastable monoclinic form sustains an irreversible martensitic transition to β between 1120 and 1220 °C, thus forbidding any application despite a low expansion coefficient ($+2.6 \times 10^{-6}\ K^{-1}$) [4,10]. However, the hafnium analogue ($+2.9 \times 10^{-6}\ K^{-1}$) does not undergo the α–β transition before decomposition, around 1500 °C.

Orthorhombic β-$Zr_2O(PO_4)_2$ (β-ZP, Fig. 1d) features ZrO_7 pentagonal bipyramids that form chains by edges-sharing along the *a*-axis [11]. The non-phosphate oxygen builds a linear unit with two zirconium atoms. The ultra-low expansion of β-ZP ($+1.5 \times 10^{-6}\ K^{-1}$) has been discovered in 1985 [12] and explained recently by a dual mechanism involving a reduction of the cell cavities under the effect of inter-cations repulsions and a transverse rocking of the oxygen atoms in twofold coordination [13]. Also thermally and chemically stable, it is undoubtedly the most useful among zirconium phosphates regarding applications (refractories, composites with SiC fibers and dimensionally stable components up to 1550 °C). It has been commercialized since the late 1990s, mainly under porous form. Paradoxically, β-ZP remains far less studied by the academic community than the NZP's and

---

* Corresponding author. Tel.: +33 1 53 73 79 46; fax: +33 1 46 34 74 89.
E-mail address: gilles.wallez@upmc.fr (G. Wallez).

0025-5408/$ – see front matter © 2010 Elsevier Ltd. All rights reserved.
doi:10.1016/j.materresbull.2010.08.005

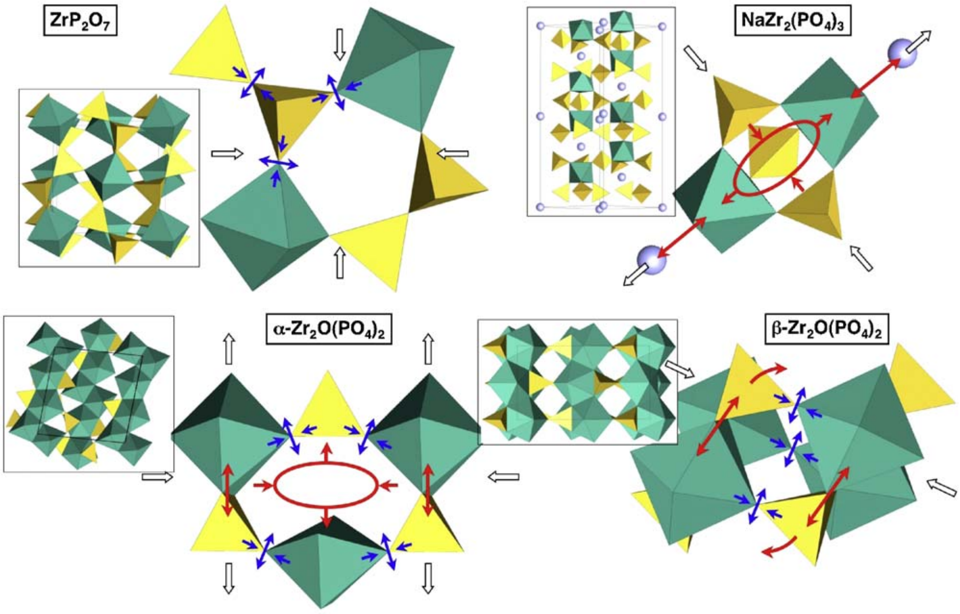

Fig. 1. From top left (a) to bottom right (d): Negative thermal expansion mechanisms in the zirconium phosphates: blue arrows show polyhedra or oxygen rocking, red arrows ring-like deformations or atomic movements resulting from inter-cations repulsions, black arrows show the global expansion/contraction. Artwork made with Balls & Sticks [17]. (For interpretation of the references to color in text, the reader is referred to the web version of the article.)

diphosphate. To this date, the only known isotypes are $U_2O(PO_4)_2$ and $Th_2O(PO_4)_2$ [14] (U^{IV}: 1.09 Å, Th: 1.14 Å (est.), Zr^{IV}: 0.92 Å in sevenfold coordination [15]) which exhibit a remarkable negative expansion (resp. -1.2 and $-1.5\ 10^{-6}\ K^{-1}$ [16]). For safety concerns, the main interest of these compounds is to evidence a clear relationship between structural and thermal properties: the bigger the cation, the stronger the rocking, the lower the expansion. In these compounds, the steric effect of the cation consists in giving its oxygen neighbors enough space to rock independently of the other ones, even if the latters are blocked by a higher coordinence (as it is the case in β-ZP). According to this mechanism, and at variance with the rigid units model that prevails for global polyhedra rocking, substitutions of cations with higher radii for Zr^{IV} or even P^V could be an attractive way to bring the thermal expansion of β-ZP closer to zero. Whereas the literature is surprisingly scarce on this subject, the present work reports a wide spectrum of experiments and proposes conclusions based upon structural criteria about the possibility to improve this material.

2. Experimental

2.1. Syntheses

Wet route syntheses are carried out from $NH_4H_2PO_4$ (Sigma–Aldrich, 98.5%), $ZrOCl_2{\cdot}8H_2O$ (Sigma–Aldrich, 99.5%) and adequate soluble salts of cations for substitutions weighted in proportions corresponding to the expected final formulas, then dissolved in distilled water and mixed to obtain gels. We observed that remaining chlorides replace the phosphates as counteranions and provoke their loss and formation of ZrO_2 during annealing. So, the gels have to be washed and separated by centrifugation several times until elimination of Cl^- anions from the supernatant ($AgNO_3$ test). The precursors are then dried at 300 °C and annealed at various temperatures depending on the composition. For dry route syntheses, $ZrO(NO_3)_2{\cdot}2H_2O$ (Prolabo, 99%) is preferred to ZrO_2 for its higher reactivity. Specific informations are reported in Table 1.

Table 1
Summary of the synthesis experiments for substituted forms of β-ZP. WR and DR refer to wet and dry routes.

Expected substitution	Specific reagents	Heat treatment	Result
$Ce^{IV} \rightarrow Zr^{IV}$, WR	CeO_2 99.9% [a] in HNO_3 1 M	1200–1500 °C air or O_2	β-ZP (683.87(7) Å^3) + $Ce^{III}PO_4$
5% $Ce^{IV} \rightarrow Zr^{IV}$, WR	id.	1200–1500 °C air or O_2	β-ZP (683.92(8) Å^3) + $Ce^{III}PO_4$
$As^V \rightarrow P^V$, WR or DR	$As_2O_5{\cdot}xH_2O$ 99.99%[a]	1100 °C	α-Form $Zr_2O(AsO_4)_2$, see Table 2
1–12% $V^V \rightarrow P^V$, WR	NH_4VO_3 99% [b] in HNO_3 0.1 M	1200 °C	See Section 3.2
5% $Nb^V \rightarrow P^V$, WR	$NbCl_5$ 99% [a] in EtOH	1400 °C	β-ZP (683.80(9) Å^3) + $Nb_2Zr_6O_{17}$
7.3% $Nb^V \rightarrow P^V$, DR	Nb_2O_5 99.8% [a], 5 mass% + β-ZP	1400 °C	β-ZP (683.94(7) Å^3) + $Nb_2Zr_6O_{17}$
5% $Mg^{II} \rightarrow Zr^{IV}$	$Mg(NO_3)_2{\cdot}6H_2O$ 99%[a]	1200–1400 °C	β-ZP (684.04(8) Å^3) + unidentified phase
5% $W^{VI} \rightarrow P^V$, WR	H_2WO_4 99% [a] in NH_3 2 M		
5% $Tb^{III} \rightarrow Zr^{IV}$	Tb_4O_7 [d] in HNO_3 1 M	1400 °C	β-ZP (684.05(3) Å^3) + $TbPO_4$ + unidentified phase
5% $W^{VI} \rightarrow P^V$, WR	H_2WO_4 99% [a] in NH_3 2 M		
5% $Sc^{III} \rightarrow Zr^{IV}$	Sc_2O_3 99.9% [a] in HNO_3 1 M	1400 °C	β-ZP (684.33(3) Å^3) + $ScPO_4$ + unidentified phase
5% $W^{VI} \rightarrow P^V$, WR			
5% $Si^{IV} \rightarrow P^V$	$SiC_8O_4H_{20}$ (TEOS), 98%[c]	1250 °C	β-ZP (684.04(8) Å^3) + unidentified phase
5% $W^{VI} \rightarrow P^V$, WR	H_2WO_4 99% [a] in NH_3 2 M	1450 °C	id. + ZrO_2

[a] Sigma–Aldrich.
[b] Merck.
[c] Fluka.
[d] Laboratory preparation.

Table 2
Cell parameters (Å,°) and thermal expansion coefficients 20–750 °C (°C^{-1}) for α-$Zr_2O(PO_4)_2$ [9,10] and α-$Zr_2O(AsO_4)_2$ (this work).

	a/α_a	b/α_b	c/α_c	β	$V/\alpha_l = (\alpha_V)/3$
α-$Zr_2O(PO_4)_2$	10.2726(6)	6.5957(3)	10.0665(5)	95.433(3)	679.00(6)
	1.7	−1.1	7.0		2.6
α-$Zr_2O(AsO_4)_2$	10.3547(5)	6.8345(3)	10.3568(4)	95.383(2)	729.71(6)
	1.3	−1.2	7.6		2.5

2.2. Analytical methods

The products are identified by X-ray diffraction on a Panalytical X'Pert Pro apparatus. The diffractometer is equipped with an Anton-Paar furnace for high temperature X-ray diffraction. The cell parameters are refined by Rietveld analysis [18]. A particular attention is paid to the cell parameters and volume of the β-ZP phase in order to observe even faint chemical variations of the material. ^{31}P and ^{51}V solid state nuclear magnetic resonance (NMR) spectra were recorded on a Bruker Avance III 300 spectrometer with a magnetic field of 7 T corresponding to 300.29 MHz for ^{1}H, 121.56 MHz for ^{31}P and 78.93 MHz for ^{51}V. A Bruker triple resonance Magic Angle Spinning (MAS) probe was used with spinning frequencies of either 14 or 11.5 kHz. ^{31}P and ^{51}V spectra were respectively referenced to H_3PO_4 85% and $VOCl_3$.

3. Results and discussion

3.1. Isovalent substitution for Zr^{IV}

Besides actinides, the only tetravalent cations bigger than Zr^{IV} are Pb^{IV} (0.95 Å) and Ce^{IV} (1.06 Å). The former has to be dismissed because of its volatility which makes it unsuitable for high temperature applications. The attempts to elaborate $Ce^{IV}{}_2O(PO_4)_2$ under air by dry and wet routes only yield monazite $Ce^{III}PO_4$, known to be a highly stable mineral. A Zr/Ce = 95/5 mol ratio precursor gives likewise a mixture of $CePO_4$ and unsubstituted β-ZP. Similar experiments made under oxygen flow give the same results. In a previous work, we evidenced the thermal decomposition of the first known cerium IV phosphate ($Ce^{IV}{}_4(PO_4)_4(P_2O_7)$) into a mixture of $Ce^{III}PO_4$ and $Ce^{III}(PO_3)_3$ around 850 °C [19], also accounting for the extreme difficulty to accommodate Ce^{IV} in an anhydrous phosphate environment [20]. So, isovalent substitutions for Zr^{IV} seem to be limited to the previously known actinide-based isotypes. Besides, stable tetravalent cations bigger than Zr^{IV} simply do not exist.

3.2. Isovalent substitution for P^{V}

Likewise, the substitution of a bigger pentavalent cation (As^{V} (0.475 Å), V^{V} (0.495 Å) or Nb^{V} (0.62 Å)) for P^{V} (0.31 Å) in the tetrahedral site could conceivably reduce the thermal expansion, like for V-substituted ZrP_2O_7 [6]. We obtain inedite $Zr_2O(AsO_4)_2$ by both wet and dry routes and find it to be isotype with α-ZP (monoclinic *I*2/*m*). This allows supposing that a continuous solid solution exists between the phosphate and the arsenate. Cell parameters and thermal expansion coefficients for both compounds are reported in Table 2: the arsenate is found to have also a low expansion, but not significantly lower than that of the phosphate. α-$Zr_2O(AsO_4)_2$ has been heated in search for a β form, but decomposition occurs around 1300 °C, before a transition could be observed. This suggests that a bigger pentavalent cation in the tetrahedral site stabilizes the α form, whereas a compared study of α-ZP and α-HP (Hf^{IV} homologue) evidences an inverse steric effect of the tetravalent cation [9].

Although very similar in size to As^{V}, V^{V} is found to substitute only in small amounts for P^{V}: ZrO_2 and $Zr(P,V)_2O_7$ diffraction peaks appear around 12 or 16%, likewise, as shown on Fig. 2, the increase of the cell volume tend to reduce with V rate. Even within the solubility limits, the color of the samples evolves gradually from pale yellow to amber with the vanadium rate.

As a rule of thumb, considering the nearly equal radii of V^{V} and As^{V} on the one hand, and the similarity of the densities of α-ZP and β-ZP ($\Delta\rho = 0.7\%$) on the other hand, the β-$Zr_2O((P,V)O_4)_2$ cell volume should evolve roughly like for the α-$Zr_2O((P,As)O_4)_2$ solid solution (Table 2), at about 0.5 Å^3/% (Fig. 2, red line). Actually, the experimental slope is lower than expected, thus calling for a thorough analysis of the substitution mechanism.

The ^{31}P NMR spectrum of pure β-ZP shows a strong single peak at −23.1 ppm (Fig. 3) that corresponds to the unique P site. This

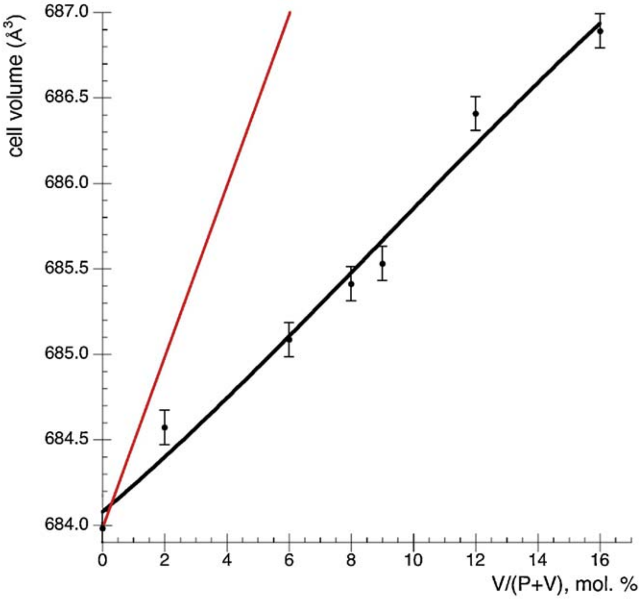

Fig. 2. Black plot: experimental variation of the β-ZP cell volume vs. vanadium rate. Red line corresponds to the expected variation. (For interpretation of the references to color in text, the reader is referred to the web version of the article.)

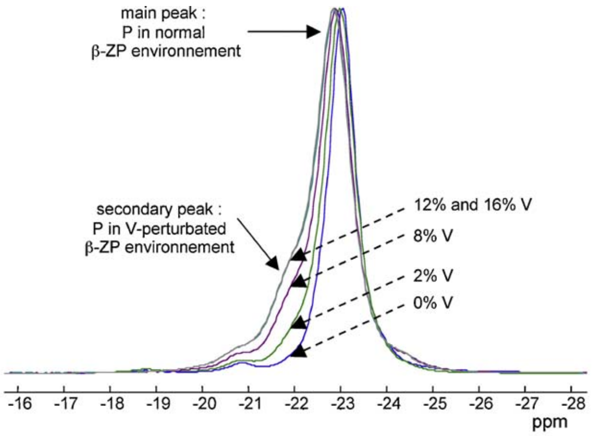

Fig. 3. ^{31}P NMR spectra of pure and V-substituted β-ZP.

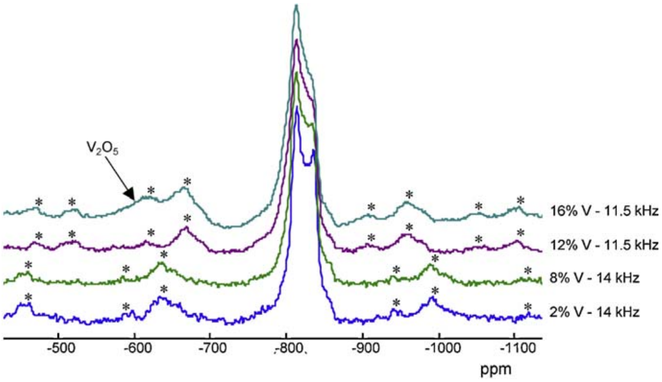

Fig. 4. ^{51}V NMR spectra of V-substituted β-ZP. *Indicate spinning side bands.

value is in good agreement with the 25 ppm reported by Clayden for a P(–O–Zr)$_4$ environment [21]. The peak shifts progressively with the increasing V rate, while a shoulder grows up around −22 ppm, probably due to moderate deformation of the P site caused by the substitution of the neighboring P's by a V (shortest $d = 3.95$ Å). Both peaks cease to evolve between 12 and 16 V%, accounting for the already observed saturation. Even at high V%, neither an increase of the spinning side bands or a strong decrease of the relaxation delay is observed on ^{31}P spectra, indicating the absence of detectable paramagnetic species in the samples, meaning that Vanadium is only as V^V.

On ^{51}V NMR (Fig. 4), the central peak is strongly shifted compared to V_xO_y poly-oxo-vanadates, but such a value is not unusual for V in a zirconium oxide environment [22]. Its splitting (−813 and −834 ppm) can be ascribed to the second-order nuclear quadrupole interaction caused by the strong asymmetry inducing electric field gradient in the host tetrahedron (in pure β-ZP, the edge shared with Zr results in a low O–P–O angle of 96.8°). On both sides of the main peak, spinning side bands are observed at multiples of the spinning frequency. One can notice that at 16 V% a broad peak appears around −620 ppm attributable to a secondary amorphous vanadate phase. The spinning frequency was changed to better see this peak.

Whereas the partial insertion of V^V appears undoubtful on the basis of XRD and NMR, it seems however poorly stable in this environment: the prolonged annealing (1200 °C, 10 h) of an 8 V% dried sample results in a 1.5% weight loss, to be compared to its nominal 2.3 mass% assay in V_2O_5 (the weight of a pure β-ZP sample heated in the same conditions remains unchanged). In the same time, weak diffraction peaks of an unknown phase appear, accounting for a decomposition, probably due to the evaporation of vanadium oxide. It seems probable that this loss also occurs during the synthesis, thus explaining the volumic anomaly observed, but it is difficult to measure precisely the real V rate in the β-ZP phase of these samples and to conclude about possible vacancies left by the P/V_2O_5 loss and affecting the cell volume. Nonetheless, no significant variation of the coefficient of thermal expansion ($1.5 \leq \alpha \leq 1.6 \times 10^{-6}$ K^{-1}) in the solubility domain (0, 2, 6, 8, 10 and 12 V%) was measured by high temperature XRD and Rietveld analysis.

On the opposite, vanadium has remarkable structural effects on the material. As shown in Fig. 5, the crystallization (DTA measurements) and the α–β transition (XRD measurements) occur at lower temperatures and, concerning the latter, within a reduced thermal range when the V rate increases. Even in faint amounts, vanadium also enhances the crystallinity of the β form, which diffraction peaks are narrower (Fig. 6). At last, whereas pure β-ZP needs to be ground several times and annealed up to 1400 °C to eliminate residual ZrO_2 and ZrP_2O_7, samples with 2 V% treated at 1000 °C appear single-phase.

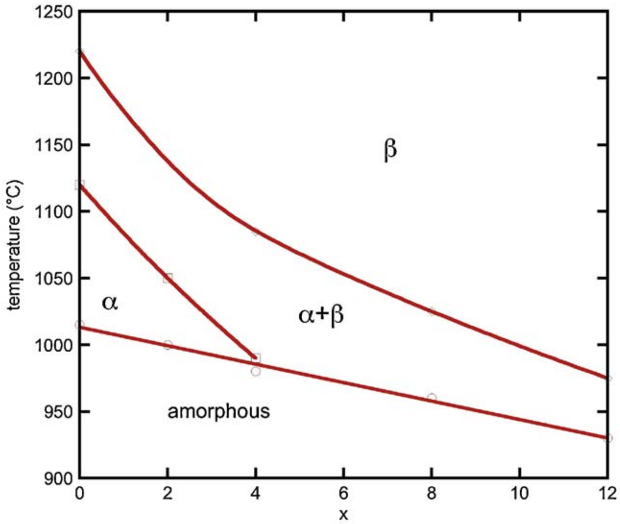

Fig. 5. Amorphous, α, β and coexistence domains of $Zr_2O((P,V)O_4)_2$ solid solutions. Relative amounts of both phases are inferred from the scale factors (Rietveld analysis, α:β = 50:50 mixture used as standard).

Improved diffusion mechanisms, either through a vanadium-rich liquid phase (corresponding to the amorphous peaks of ^{51}V NMR) or involving structural vacancies can be responsible for these beneficent effects that could allow the elaboration of well-crystallized β-ZP refractories at moderate temperature.

The effect of Nb^V was mentioned in 1987 by Yamai et al., who observed a slight increase of the cell volume for a β-ZP sintered at 1400 °C in addition with 5 mass% Nb_2O_5 [23]. Considering that the ionic radius of Nb^V is intermediate between those of P^V and Zr^{IV}, this would account for a partial substitution of Nb^V for P^V. However, this experiment, made again in the same conditions, gives us a sintered composite (89% compact) of unmodified β-ZP and $Nb_2Zr_6O_{17}$. Despite Nb^V sometimes occurs in fourfold coordination, it could be too bulky to take place into the β-ZP structure.

3.3. Aliovalent substitutions

Simultaneous substitutions for Zr^{IV} and P^V by cations of different oxidation states are also conceivable, provided that the

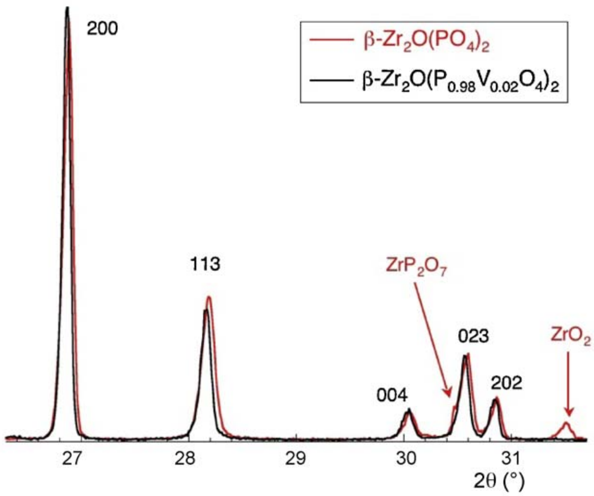

Fig. 6. Zoom on the XRD powder patterns of 0 V% β-ZP (heated 1300 °C, red) and 2 V% β-ZP (heated 1000 °C, black). Note the broadening of the 0 V% peaks (*HWHM* = 0.12°) compared to those of the 2% sample (0.10°), and the presence of residual ZrP_2O_7 and ZrO_2 in the former. (For interpretation of the references to color in text, the reader is referred to the web version of the article.)

global charge of the cell remains unchanged. Various schemes have been considered, involving size-compatible bivalent and trivalent cations in substitution for Zr^{IV} (penta- and hexavalent cations are all smaller), while W^{VI} has been chosen to replace P^{V} for its thermal and chemical stability as well as its compatibility with a tetrahedral environment. As shown in Table 1, each of these potential dopants eventually gives an unwanted compound in addition to pure β-ZP, meaning a failure of the substitution.

Kim et al. recently reported the elaboration of single-phase β-ZP doped with 1–10% Tb^{III} in substitution for Zr^{IV} and presented the diffraction pattern of the 3% Tb sample [24]. The authors gave no informations about the cell parameters, but a careful examination evidences the diffraction peaks of xenotime-like $TbPO_4$ at $2\theta = 19.6^\circ$ and 25.6°, like for our sample, leading to suppose that the substitution was not really effective. The light emission peaks they reported result undoubtedly of *f*-level transitions of Tb^{III}, but keeping in mind their low sensitivity to the environment, one must remark that they also match with those of $TbPO_4$.

Another aliovalent substitution has been thought up for the tetrahedral site only, to be partly occupied by equal amounts of Si^{IV} and W^{VI}, both bigger than P^{V}. This attempt is also unsuccessful.

The systematic failures of aliovalent substitutions can be understood on structural bases. First, one should consider that the ZrO_7 polyhedra are paired by vertices through Zr–O–Zr linkages (Fig. 1d): to our knowledge, such oxo units occur only for high-valence cations (≥IV); otherwise (*i.e.* for a $M^{III}O_7$ polyhedron) the distribution of bond strengths would be exceedingly assymmetric (1 v.u. for the oxo bond and only 2 v.u. to be shared between the 6 other ones). In these conditions, no efficient aliovalent substitution can be made for Zr^{IV}. This calls for a comparison with the NZP structure, in which Zr^{IV} occupies an independent octahedron and can be replaced by any size-compatible cation with valency III to V, thus allowing an easy control of the thermal expansion. Another structural peculiarity of β-ZP should be put forward for understanding the failure of the simultaneous substitution of Si^{IV} and W^{VI} for P^{V}: the edge-sharing between ZrO_7 and PO_4. Such a feature is rather uncommon between cations with so high charges, and increased Coulombic interactions, like those caused by W^{VI} for example, could make it impossible. Indeed, to our knowledge, a WO_4 tetrahedron never shares an edge with a M^{IV}-based polyhedron. At variance once again, W^{VI} can replace ($Na^+ + P^V$) in NZP to give orthorhombic $Zr_2(PO_4)_2(WO_4)$, a somewhat different structure in which the tungstate tetrahedra are corner-connected [25,26]. It is also nowadays used in commercial ultra-low expansion materials.

4. Conclusion

Despite the substitution of bigger cations in β-ZP could appear as an appealing way to reduce its thermal expansion, very few isovalent species proved to be compatible: Th^{IV} and U^{IV} for Zr; V^{V} for P in low amounts because of its volatility, and As^{V} that only yields of α-form. Either unsafe, volatile or chemically unstable, the isovalent cations do not give useful materials, but vanadium improves the crystallinity and reduces the transition point significantly. This could be an interesting way to elaborate this material at a lower cost. Aliovalent substitutions are very probably forbidden by the structural peculiarities of the material, thus leaving no clear way to increase its intrinsic resistance to thermal shocks. To our opinion, adjusting extrinsic microstructural parameters such as porosity, secondary phases or microcracks is a more promising way to improve β-ZP, whereas the bulk itself should be considered as stuck to the archetype formulation. Considering its technological importance, such attempts as ours to modify the composition might have been carried out previously and have given similar results, therefore remained unreported. So, we hope this in-depth study on β-ZP will give ceramists a clearer insight on its crystal–chemical properties and help them saving time and efforts in their works on this valuable material.

Acknowledgments

This work was funded by the French program MATINEX (CNRS-CEA). The authors are very grateful to Eléonore Noussan and Laetitia Corde, students of Chimie-ParisTech for their precious help during their training period and to Dr. Christel Gervais-Stary (LCMCP) for her comments on the NMR spectra.

Appendix A. Supplementary data

Supplementary data associated with this article can be found, in the online version, at doi:10.1016/j.materresbull.2010.08.005.

References

[1] R. Roy, D.K. Agrawal, H.A. McKinstry, Annu. Rev. Mater. Sci. 19 (1989) 59–81.
[2] A.W. Sleight, Inorg. Chem. 37 (1998) 2854–2860.
[3] D.E. Harrison, H.A. McKinstry, F.A. Hummel, J. Am. Ceram. Soc. 37 (1954) 277–280.
[4] J. Alamo, R. Roy, J. Am. Ceram. Soc. 67 (1984) 80–82.
[5] N. Khosrovani, V. Korthuis, A.W. Sleight, T. Vogt, Inorg. Chem. 35 (1996) 485–489.
[6] V. Korthuis, N. Khosrovani, A.W. Sleight, N. Roberts, R. Dupree, W.W. Warren, Chem. Mater. 7 (1995) 412–417.
[7] J.P. Boilot, J.P. Salanié, G. Desplanches, D. Le Potier, Mater. Res. Bull. 14 (1979) 1469–1477.
[8] D.K. Agrawal, C.Y. Huang, H.A. McKinstry, Int. J. Thermophys. 12 (1991) 697–710.
[9] G. Wallez, J.P. Souron, M. Quarton, Solid State Sci. 8 (2006) 1061–1066.
[10] G. Wallez, D. Bregiroux, M. Quarton, J. Solid State Chem. 181 (2008) 1413–1418.
[11] W. Gebert, E. Tillmanns, Acta Crystallogr. B31 (1975) 1768–1770.
[12] I. Yamai, T. Ota, J. Am. Ceram. Soc. 68 (1985) 273–278.
[13] G. Wallez, S. Launay, J.P. Souron, M. Quarton, E. Suard, Chem. Mater. 15 (2003) 3793–3797.
[14] N. Dacheux, N. Clavier, G. Wallez, M. Quarton, Solid State Sci. 9 (2007) 619–627.
[15] R.D. Shannon, Acta Crystallogr. A32 (1976) 751–767.
[16] G. Wallez, S. Launay, M. Quarton, N. Dacheux, J.L. Soubeyroux, J. Solid State Chem. 177 (2004) 3575–3580.
[17] S.J. Kang, T.C. Ozawa, Balls & Sticks, V.1.51, 2004.
[18] J. Rodriguez-Carvajal, FULLPROF.2k: Rietveld, Profile Matching and Integrated Intensity Refinement of X-ray and Neutron Data, V 1.9c, Laboratoire Léon Brillouin, CEA, Saclay, France, 2001.
[19] M. Nazaraly, G. Wallez, C. Chanéac, E. Tronc, M. Quarton, J.P. Jolivet, J. Phys. Chem. Solids 67 (2006) 1075–1078.
[20] D. Bregiroux, O. Terra, F. Audubert, N. Dacheux, V. Serin, R. Podor, D. Bernache-Assollant, Inorg. Chem. 46 (2007) 10372–10382.
[21] N.J. Clayden, J. Chem. Soc. Dalton Trans. 8 (1987) 1877–1881.
[22] J.R. Sohn, S.G. Cho, Y.I. Pae, S. Hayashi, J. Catal. 159 (1996) 170–177.
[23] I. Yamai, T. Ota, J. Am. Ceram. Soc. 70 (1987) 585–590.
[24] S.W. Kim, T. Masui, H. Matsushita, N. Imanaka, Chem. Lett. 38 (2009) 1100–1101.
[25] J.S.O. Evans, T.A. Mary, A.W. Sleight, J. Solid State Chem. 120 (1995) 101–104.
[26] T. Isobe, T. Umezome, Y. Kameshima, A. Nakajima, K. Okada, Mater. Res. Bull. 44 (2009) 2045–2049.